JOURNAL OF GEOPHYSICAL RESEARCH, VOL. 113, B11201, doi:10.1029/2008JB005731, 2008

Click Here for Full Article

Phreatomagmatic explosions of rhyolitic magma: Experimental and field evidence

A. Austin-Erickson,[1] R. Büttner,[2] P. Dellino,[3] M. H. Ort,[1] and B. Zimanowski[2]

Received 1 April 2008; revised 22 July 2008; accepted 31 July 2008; published 4 November 2008.

[1] Experimental studies on explosive molten fuel-coolant interaction (MFCI) using basaltic melt compositions and water as the coolant have provided insight into the physical processes of basaltic and andesitic phreatomagmatic volcanism. Abundant field evidence indicates that rhyolitic and dacitic phreatomagmatism occurs in nature, but it has not been possible until now to generate laboratory MFCI explosions from the interaction between high-silica melts and water under laboratory conditions. The high viscosity of these melts apparently prevents formation of an effective hydrodynamic premix of melt and water, the documented precursor of experimental explosive MFCI caused by mafic melts. Our new experiments utilized samples from a rhyolitic tuff ring volcano in Mexico (Tepexitl). An experimental approach was developed, in which premixing conditions were generated by mechanical deformation of the melt, leading to brittle-type fragmentation at the melt-water interface. Physical measurements recorded during laboratory explosion provide quantitative evidence for rhyolitic explosive MFCI. Additionally, a comparison of experimentally produced particles with natural ones from Tepexitl deposits show nearly identical chemical/mineralogical composition, grain size, and grain morphology. Detailed textural analysis confirmed the presence of phreatomagmatically produced particles in both experimental and natural analog particles. The results from this series of experiments indicate that under natural conditions, stress-induced magma fracturing can lead to a critical magma-water-interface growths and trigger phreatomagmatic explosions of high-silica magma. The water source for these eruptions may include shallow aquifers, surface water bodies, strong precipitation, and intrusion into ice or wet, unconsolidated sediments.

Citation: Austin-Erickson, A., R. Büttner, P. Dellino, M. H. Ort, and B. Zimanowski (2008), Phreatomagmatic explosions of rhyolitic magma: Experimental and field evidence, *J. Geophys. Res.*, *113*, B11201, doi:10.1029/2008JB005731.

1. Introduction

[2] Phreatomagmatic explosions [*Zimanowski*, 1998] represent the most energetic response to magma-water interactions, also called explosive molten-fuel coolant interactions (MFCI) in technical processes (increasingly used by volcanologists). Driving these explosions is the efficient conversion of thermal energy from the rising magma into mechanical energy, mainly shock waves, which travel from the locus of explosion into the surrounding magma and host rocks, causing intensive fragmentation. Maar volcanoes and tuff rings, which dominate the morphology of phreatomagmatic centers, are described by many authors to originate from the accumulation of pyroclastic ejecta during these high-energy, downward penetrating eruptions [e.g., *Houghton and Schmincke*, 1986; *Lorenz*, 1985, 1986, 1987; *White*, 1991].

[3] In the case of basaltic and andesitic magma compositions, the physics of phreatomagmatic explosions have been described and the resultant ash experimentally verified to be the result of MFCI leading to a thermohydraulic explosion [*Wohletz*, 1983, 1986; *Zimanowski*, 1998; *Zimanowski et al.*, 1997a; *Büttner and Zimanowski*, 1998; *Büttner et al.*, 1999; *Morrisey et al.*, 2000]. The initial phase of thermohydraulic explosions in these more mafic magma compositions is the "premix" formation of water domains in the liquid host magma [*Zimanowski et al.*, 1997b]. The critical parameter that governs the behavior of the premix is the size of interfacial area between magma and water per unit volume produced per time unit. During experiments with basaltic melt, thermohydraulic explosions could only be generated if a critical magma-water interface/volume ratio of about 1 (m^2/m^3) was produced within 1 s [*Büttner and Zimanowski*, 1998].

[4] The hydrodynamic energy (resulting from the differential flow speed of a volume of one liquid within a volume of another liquid) needed for the production of an explosive premix depends on the material properties of the liquids and

[1] Department of Geology, Northern Arizona University, Flagstaff, Arizona, USA.
[2] Physikalisch Vulkanologisches Labor, Universität Würzburg, Würzburg, Germany.
[3] Dipartimento Geomineralogico, Università Degli Studi di Bari, Bari, Italy.

0148-0227/08/2008JB005731$09.00

the system geometry. For near-surface volcanism, the range of thermal properties, density, interfacial tension, and mingling geometry is quite limited (less than an order of magnitude). However, the range of magma viscosities exceeds 6 orders of magnitude. Studies on hydrodynamic mingling have demonstrated that the viscosity of host magma represents the most important parameter controlling the generation of interfacial surface, with higher viscosities requiring more hydrodynamic energy to react explosively with water [*Zimanowski and Büttner*, 2003; *Zimanowski et al.*, 2004]. To date, it has not been possible to generate experimental thermohydraulic explosions using magmatic melt compositions with viscosities exceeding a few hundred Pa s.

[5] Field observations, however, provide abundant evidence for phreatomagmatic volcanism of high-silica magma [*Self and Sparks*, 1978]. Rhyolitic and dacitic tuff rings, tuff cones, and even maar-diatreme volcanoes have been recognized in locations around the world [*Sheridan and Updike*, 1975; *Sieh and Bursik*, 1986; *Houghton et al.*, 1987; *Heiken and Wohletz*, 1987; *Pier et al.*, 1992; *Brooker et al.*, 1993; *Campos Venuti and Rossi*, 1996; *Kazuhiko et al.*, 2002; *White and Urbanczyk*, 2002; *Lorenz and Haneke*, 2004; *Austin-Erickson*, 2007; *Carrasco-Núñez et al.*, 2007]. The possibility for rhyolitic or dacitic magma and water to form explosive premixes similar to those observed in more mafic magmas appears unlikely based on experimental evidence and the present knowledge of eruptive physics. However, efficient conversion of thermal into mechanical energy must occur to produce rhyolitic tuff rings and maars. Experiments on brittle fragmentation of magmatic melt [*Büttner et al.*, 2006] demonstrated that the mechanical strength of partially molten volcanic rock strongly decreases with increasing silica content (thus facilitating brittle fragmentation). This evidence suggests that an alternate mechanism to hydrodynamic mingling exists as a precursor to phreatomagmatic explosion: On the basis of mechanisms discussed and illustrated by *Wohletz and Heiken* [1987, 1992], this paper discusses the hypothesis that external water can be hydraulically forced into cracks that form along the margins of a rising high-silica plug, thus creating the critical interfacial surface area needed to initiate phreatomagmatic explosion. To test this hypothesis, a modified version of the experimental setup used by *Büttner et al.* [2006] was designed. A well-documented case history of a rhyolitic phreatomagmatic volcano (Tepexitl tuff ring) [*Austin-Erickson*, 2007] was selected to use as a natural analog, with selected samples from its deposits serving as the test material. A detailed textural comparison of the experimentally produced products (ash-sized particles) with natural particles from the Tepexitl deposits was conducted in the same manner as demonstrated by *Büttner et al.* [1999, 2002].

2. Volcanology of Tepexitl Tuff Ring

[6] Tepexitl volcano is a latest Pleistocene, peraluminous rhyolitic tuff ring in the Serdán-Oriental Basin, located at the eastern end of the Trans-Mexican Volcanic Belt (TMVB; Figure 1). The Serdán-Oriental Basin has served as a natural "catchment" for reworked Quaternary unconsolidated material from surrounding volcanoes during both glacial and interglacial times. The resulting mixture of fine-grained eolian and ephemeral fluvial deposits [*Siebe and Verma*, 1988] is the inferred shallow, regional aquifer through which Tepexitl magma erupted, with a high water table that reaches the surface in places during the summer rainy season [*Austin-Erickson*, 2007]. Tepexitl's well-preserved deposits and easily accessible crater rim make it an excellent location to study the fragmentation processes that presumably resulted from the interaction of rhyolitic magma with external water.

[7] *Austin-Erickson* [2007] determined that the eruption was characterized by closely timed explosive events that led to the formation of a complex stratigraphic sequence of pyroclastic deposits. At least three vents were active during the formation of Tepexitl, with temporal overlaps of both fragmentation mechanism and vent activity during a mid-eruption transitional phase. Stratigraphic evidence suggests that cone building and crater widening occurred during this transitional time, processes that likely occurred as early dome growth and associated phreatic eruptions began. As pyroclastic activity waned, the eruption appears to have evolved into passive dome extrusion. Subsequent retrogressive dome explosions, possibly triggered by a combination of incomplete degassing and external water (storm water and/or groundwater), destroyed the dome.

[8] Tepexitl juvenile material is quartz-plagioclase-biotite-sanidine-phyric rhyolite with accessory almandine. Clasts are dominated by stony rhyolite, obsidian, and banded textures, with sparse pumiceous and perlitic components. Stratigraphy is characterized by poorly cemented laminae to medium beds that encompass six unique facies (three coarse-grained facies and three fine-grained facies). Coarse- and fine-grained deposits alternate on a scale of centimeters to meters, with sharp contacts throughout the vertical sequence. Changes in dominant facies-type and degree of cohesivity of deposits define eight units, which can be more broadly grouped into a lower and upper sequence (Figure 2). A detailed evaluation of deposit characteristics (stratigraphic changes, componentry, grain size distribution, ash morphology) led to a reconstruction of eruptive dynamics over the course of Tepexitl's formation [*Austin-Erickson*, 2007].

[9] The lower sequence is defined by thinly bedded, planar to highly deformed, fine-grained-facies deposits (Figure 3) that are composed mainly of juvenile and lithic ash particles. Juvenile ash morphology (4 phi) is dominated by dense, blocky particles that commonly have surface textures consistent with both phreatomagmatic fragmentation and excess water in the crater area during eruption (stepped fractures, branching quench cracks, and pitting [e.g., *Heiken and Wohletz*, 1987; *Dellino and La Volpe*, 1995; *Büttner et al.*, 1999; *Dellino et al.*, 2001; *Zimanowski et al.*, 2003]. Upper-sequence deposits are composed of coarse-grained facies, with thicker and less coherent beds than those of the lower-sequence deposits (Figure 3). These contain abundant large blocks and little to no deformed ash beds, with very few lithic clasts. Clast lithology is dominated by glassy, dense to moderately pumiceous juvenile material. Fine ash morphologies (4 phi) lack the surface textures seen in the lower sequence, which is consistent with deposition from magmatic fragmentation events.

[10] All evidence points to early discrete phreatomagmatic blasts, which were erupted as wet, high-energy surges and resulted in a progressive deepening of the eruptive

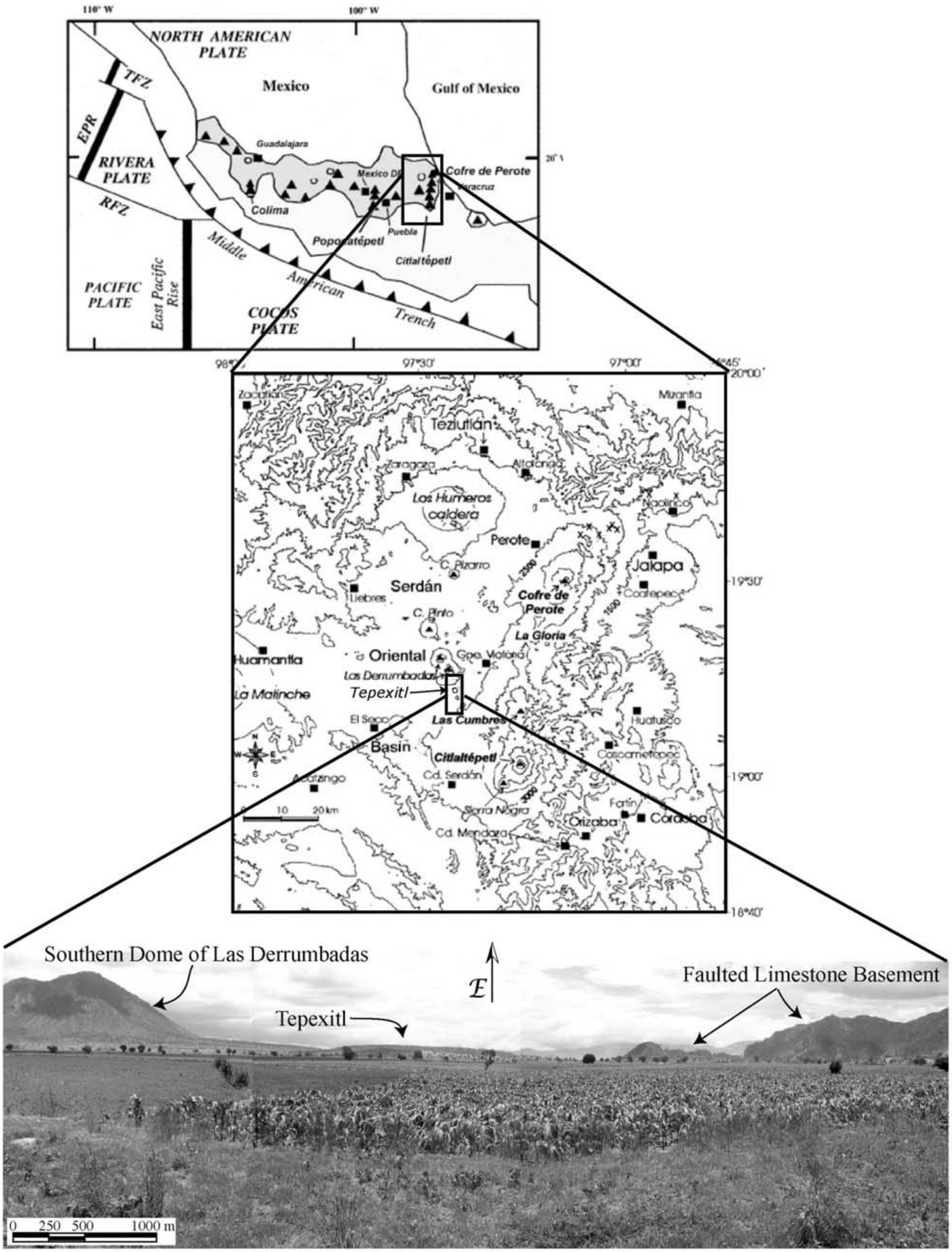

Figure 1. Location of Tepexitl tuff ring within the Serdán-Oriental Basin, a topographic low near the eastern edge of the Trans-Mexican Volcanic Belt (shown in the shaded region in the upper picture). Adapted from *Siebe et al.* [1993] and *Siebert and Carrasco-Núñez* [2002].

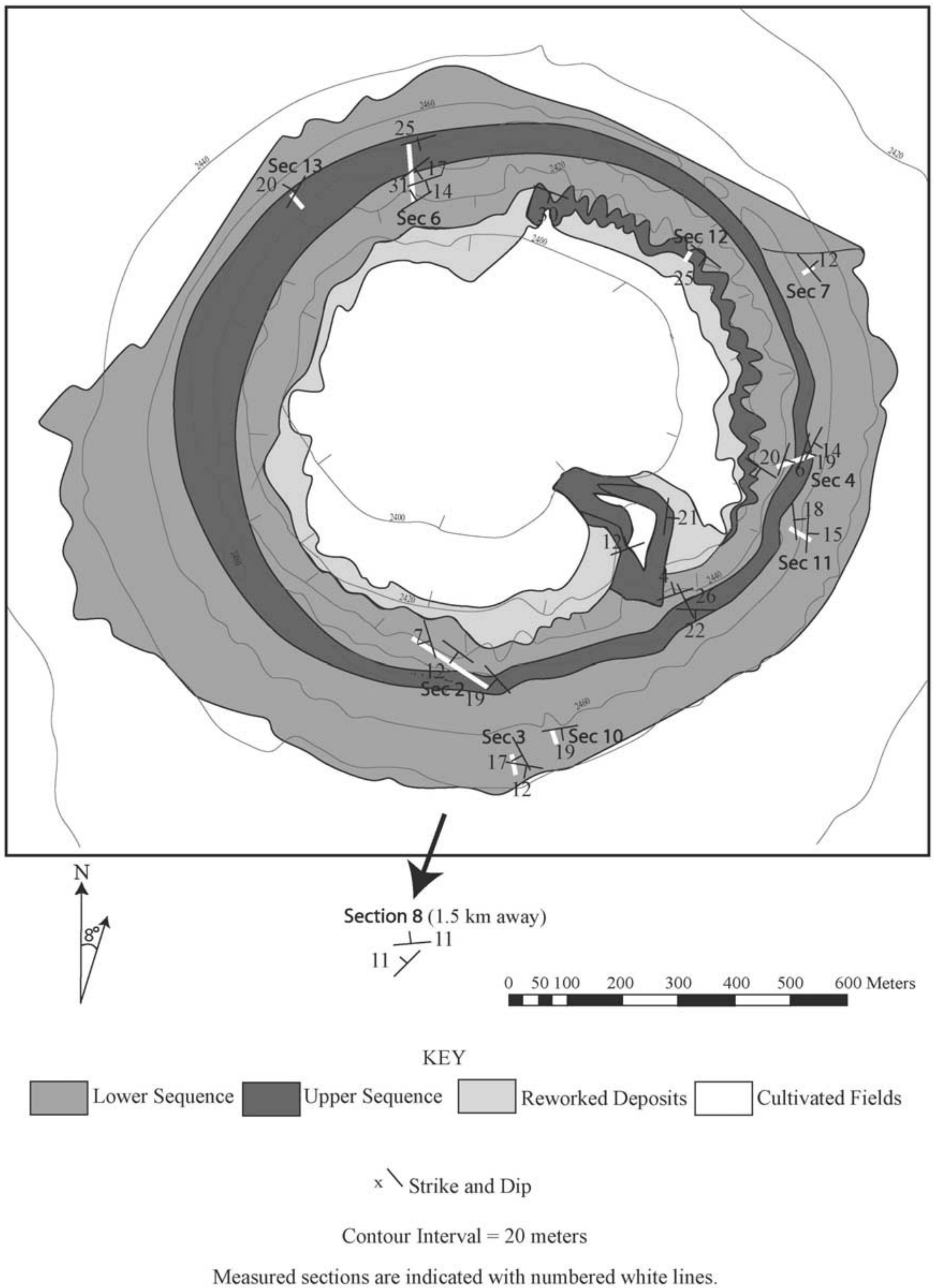

Figure 2. Simplified geologic map of Tepexitl tuff ring.

center (deposition of the lower sequence). With time, activity graded into dominantly magmatic behavior, as water supply diminished and the explosion loci became shallower (deposition of the upper sequence). Deposits associated with magmatic processes result from less energetic fragmentation and depositional mechanisms and are dominated by deposits from fallout and surges. Unit 3 of the upper sequence (Figure 3) was deposited from retrogressive dome explosions, likely triggered by a combination of incomplete degassing and external water (storm water

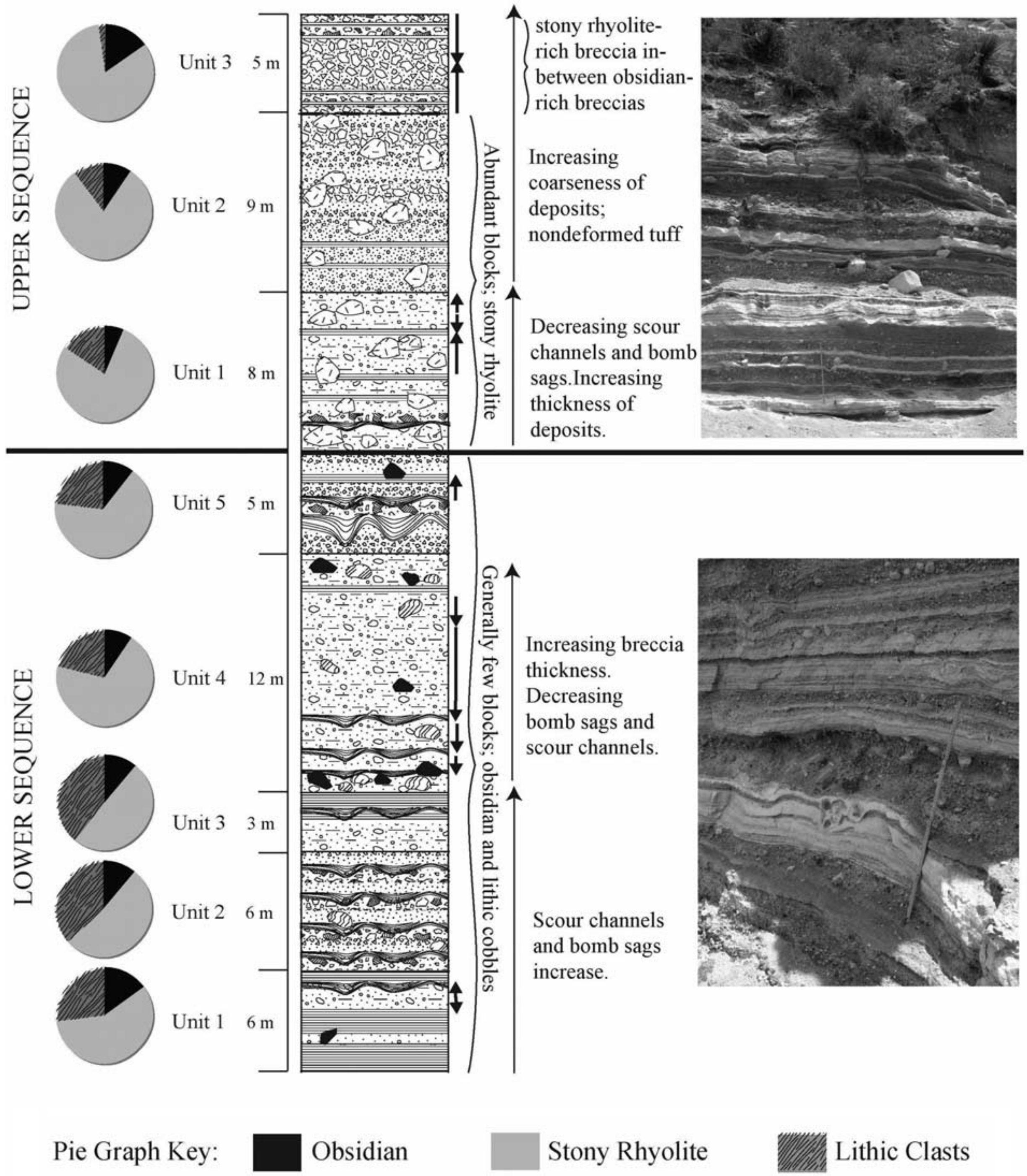

Figure 3. Generalized stratigraphic section for Tepexitl inner-crater deposits with normalized, averaged percentages of major componentry categories shown in pie graphs to the left.

and/or groundwater). No trace of the original dome morphology is exposed above the present crater floor.

3. Experimental Setup

[11] Tepexitl material served as the melt for all experimental runs at the Physikalisch Vulkanologisches Labor (PVL) at the Universität Würzburg. Preliminary melting tests were performed to investigate the behavior of both obsidian and stony rhyolite samples collected from lower-sequence Unit 2. Generally, rock samples that have been affected by hydration, weathering, and devitrification cannot be used because they vesiculate and pop up during fast melting. Owing to its melting behavior, stony rhyolite was

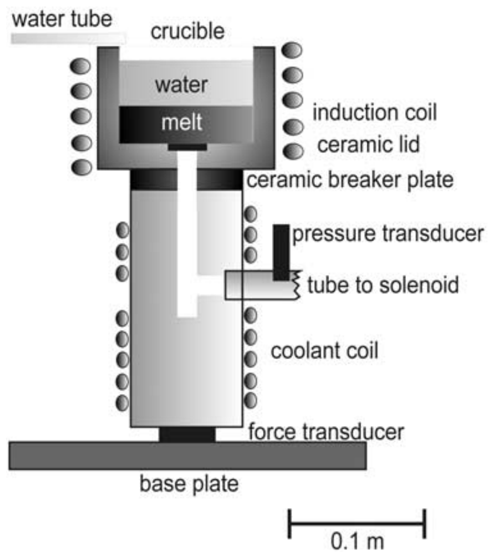

Figure 4a. Cross section of the experimental setup.

Figure 4b. Formation of first subvertical tension cracks on the surface of a melt plug in deformation, seen from above, as an example. Single frame of a video recorded during a dry explosion experiment (<20 ms before explosion) using the same setup as in the experiments described here, but with basaltic melt from the 2002 Mt. Etna eruption (Italy) at 1450 K. The internal diameter of the crucible is 10 cm. (Thanks to Jacopo Taddeucci, for his brilliant idea to use a mirror).

chosen as the experimental material for all explosive experiments.

[12] The complete experimental setup (Figure 4a) and the experimental procedure of the "dry" fragmentation experiment are described in detail by *Büttner et al.* [2006]. To create a plug of melt, 300 g of granulated Tepexitl material was placed in a cylindrical steel crucible and inductively heated. The melting process is so fast, with homogenization of material achieved in less than 1 h, that crystals and gas bubbles (if present in the material) of the original sample are preserved and only the glass/matrix portion of the material melts (disequilibrium melting). The geometry of the melt plug was adjusted so that conditions standardized by *Büttner et al.* [2006] for mass and aspect ratio were maintained. Comparing samples (taken from the melt and quenched on a metal plate) with the natural products, the melting and homogenizing procedure was adjusted. To achieve the desired state of melt, material was equilibrated at 1573 K for about 30 min and cooled down to the experimental temperature of 1473 K within 15 min. Of course we do not know the original eruption temperature, but using this method, glass composition and bubble content of samples taken from lower sequence Unit 2 ash layers could be reproduced. The thickness of the resulting melt plug was about 2 cm and its diameter 10 cm. In all runs, a fixed volume of gas pressurized to 10 MPa was connected via a solenoid to a small expansion volume with an inlet at the base of the crucible (Figure 4a), which caused a dome-like deformation of the melt plug. Once a critical deformation of the melt material is reached, first subvertical tension cracks form along the upper plug margin in response to extensional stress (Figure 4b). Subsequent brittle fragmentation and explosion is observed once the mechanical strength of the plug is exceeded (for more details, deformation calculations, and thermodynamic modeling, see *Büttner et al.* [2006]). Quasi-isothermal conditions for these "dry" runs were maintained, as the crucible was covered by an inductively heated lid, removed only seconds before the experiment.

[13] With the intention of generating MFCI explosions, the above setup was modified by mounting a solenoid-controlled water supply tube (Figure 4a), which was triggered to eject a set amount of water on top of the melt plug in the time window between 600 and 200 ms before the onset of deformation. In first approximation also quasi isothermal starting condition can be assumed in this case as the insulating vapor film (Leidenfrost Phenomenon) that forms between the water layer and the melt will initially prevent high heat transfer rates. It was presumed that during these "wet runs," the resulting stratification would result in rapid intrusion of water into the subvertical cracks as they formed during doming (Figure 5) and the pressure pulses resulting from the crack formation would be strong enough to trigger the collapse of the vapor film [*Büttner and Zimanowski*, 1998]. In all experiments, driving pressure,

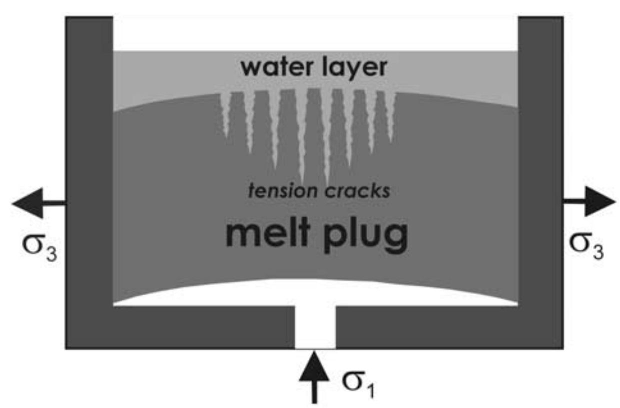

Figure 5. Schematic drawing of the experimental configuration during deformation and brittle reaction prior to explosive MFCI.

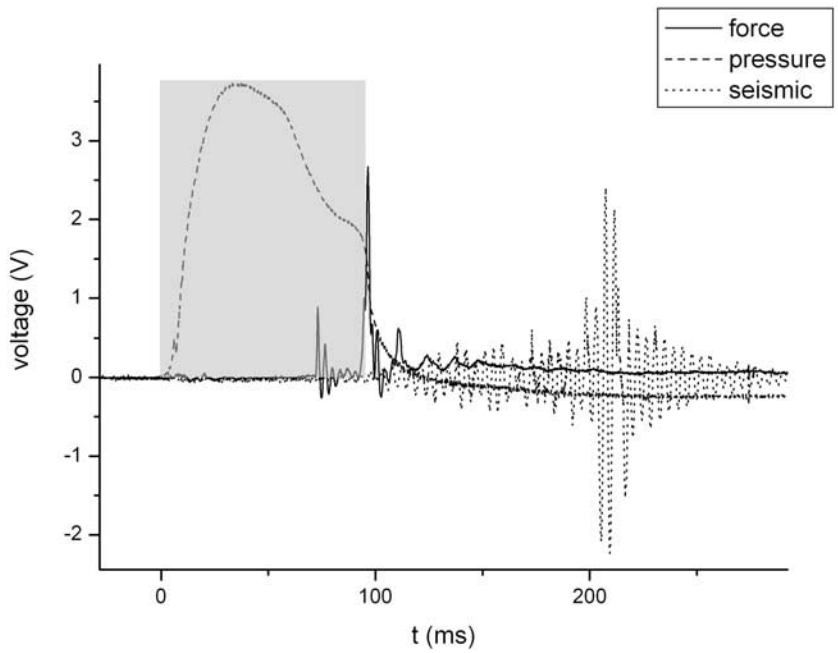

Figure 6. Strongest dry explosive run. Driving pressure [1 V = 2 MPa], repulsion force [1 V = 1 kN], and a qualitative record of the seismoacoustic air wave measured 1.8 m from the source of explosion. Shaded area marks the loading time.

repulsion force, and explosion seismoacoustics were recorded at 100 kHz. The ejection velocity was monitored using conventional (50 fps) and high-speed (500 fps) video. The newly produced particles were sampled immediately after the experiments. In addition, reference particles for passive thermal granulation [*Büttner et al.*, 1999] were produced for this study by quenching both obsidian and stony rhyolite-derived melts in a water container (TG runs).

4. Experimental Results

[14] Both experimental series resulted in explosive fragmentation of the melt plug and ejection of particles in the

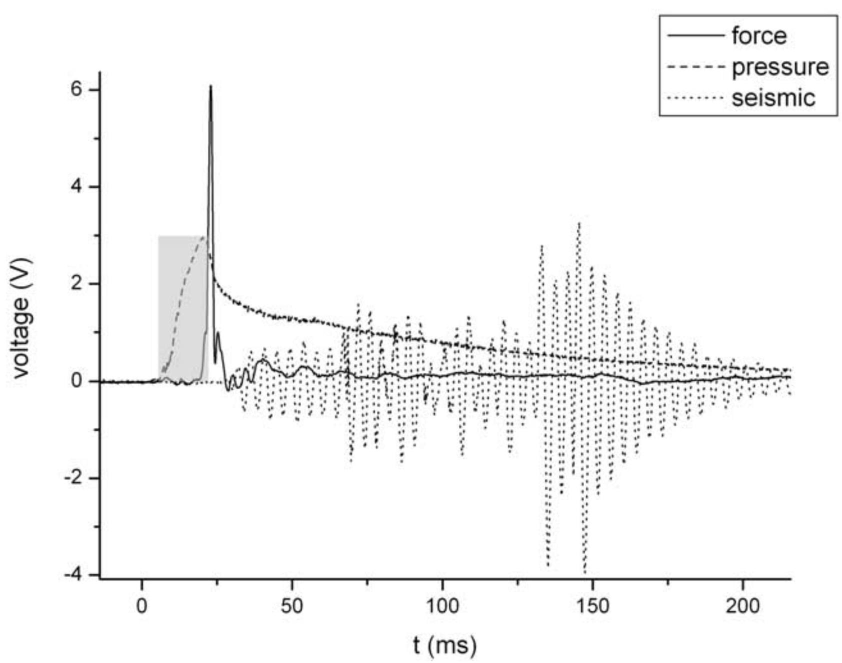

Figure 7. Strongest wet explosive run. Driving pressure [1 V = 2 MPa], repulsion force [1 V = 1 kN], and a qualitative record of the seismoacoustic air wave measured 1.8 m from the source of explosion. Shaded area marks the loading time.

Table 1. Force and Pressure History and Ejection Velocity of the Strongest Dry and Wet Experimental Runs[a]

Experiment	Peak Driving Pressure (MPa)	Loading Time Until Brittle Failure (ms)	Repulsion Force (kN)	Maximum Ejection Velocity (m/s)
DE	7.78	98.09	2.66	110
WE	5.92	19.91	6.11	250

[a]Here DE is dry experiment and WE is wet experiment. Shown in Figures 6 and 7.

grain size range of volcanic ash. The strongest explosion was observed, when a water volume of 300 ml was added on top of the melt plug, forming a water layer of about 3.8 cm thickness. A comparison of force and pressure histories and ejection velocities for the strongest dry explosive run (DE; Figure 6) and the strongest wet explosive run (WE; Figure 7) shows that much more deformational energy (proportional to the area under the pressure curve prior to the explosion onset marked by the force curve) was needed in the dry run to initiate explosion than in the wet run (Table 1). In contrast, the kinetic energy released during eruption (peak repulsion force and ejection velocity) was distinctly higher in the wet run. Because melt mass, geometry, temperature, and reservoir pressure were the same in both runs, a significant amount of thermal energy from the melt must have been converted into kinetic energy during the wet runs, as there is no other source of energy available. This evidence suggests that explosive MFCI occurred in the wet explosive runs.

5. Particle Analysis

[15] Grain-size distribution of samples primarily reflects the (deformation) energy density at fragmentation [*Zimanowski et al.*, 2003]. A comparison of grain size distributions of samples produced by magmatic (DE) and phreatomagmatic (WE) fragmentation (Figure 8) indicates that the amount of fine-grained material correlates only with the intensity of the explosions and does not appear to be affected by fragmentation mechanism: the mode of the frequency curves is very similar and only the amount of fine particles is distinctly higher in the WE sample.

[16] The most diagnostic particles for characterizing fragmentation mechanisms are juvenile glass fragments in the size range between 3 and 5 phi, as these fine ash fragments have experienced the highest fragmentation energies [*Zimanowski et al.*, 1991; *Dellino and La Volpe*, 1996; *Büttner et al.*, 2002]. Additionally, in phreatomagmatic explosions, particles that possess the ‘‘fingerprints’’ of explosive magma-water interaction can be found in this size range. Such particles are called ‘‘active’’ because they represent the part of the melt that directly interacted with liquid water at the onset of fragmentation and are represented by diagnostic surface features (e.g., stepped fractures and quenching cracks) [e.g., *Büttner et al. 1999*, 2002]. In order to understand fragmentation mechanisms of both natural and experimental explosions, the 4-phi size fraction was extracted from all analyzed samples and examined with a scanning electron microscope (SEM) using backscatter imagery (BSE). Particle characterization was accomplished by morphological examination and comparison of natural Tepexitl deposits to experimental particles from thermal granulation (TG), dry explosive (DE), and wet explosive (WE) processes. An energy dispersive spectrometer (EDS) linked to the SEM was used for checking the chemical composition of the glass particles surfaces. Naturally and experimentally produced particles have the same composition (within the accuracy of the method used), which means that experimental melting of stony rhyolite material did not significantly alter the original composition.

[17] Particles from the additionally conducted thermal granulation runs (TG) show the typical platy and cuspate morphologies (Figures 9a and 9b) [e.g., *Büttner et al.*, 2002]. Very few of these particles are present in any natural samples, which suggests that thermal granulation was not a

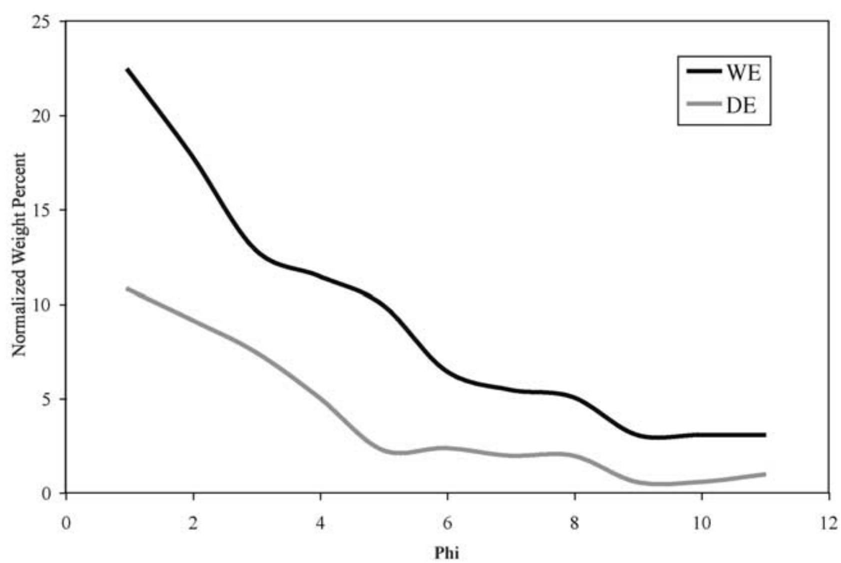

Figure 8. Grain-size distributions of the fine-grained material from the strongest wet and dry explosive experimental runs.

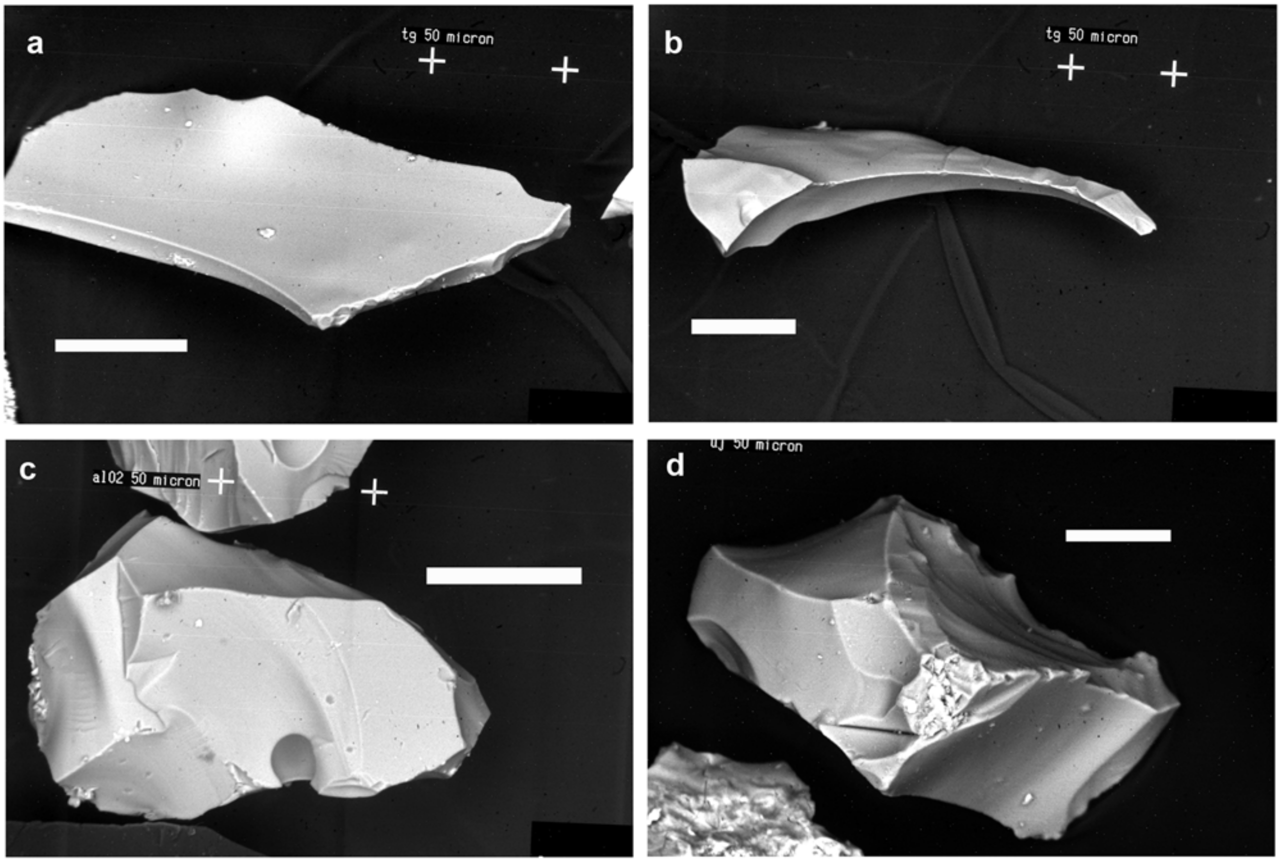

Figure 9. Ash particles (a and b) from TG experiments, (c) from DE runs, and (d) from natural sample. Scale bar is 50 μm.

significant fragmentation mechanism during the shallow water/magma interactions of Tepexitl eruptions. Material from the dry explosive runs (DE) contains primarily dense to moderately vesiculated particles with smooth, planar, or curviplanar surfaces and blocky/angular shapes (Figure 9c). These same features can be seen in Tepexitl natural samples (Figure 9d), now interpreted as products from stress-induced brittle fragmentation processes (magmatic fragmentation) [e.g., *Büttner et al.*, 2006].

[18] Experimental particles from the wet explosive runs (WE) are dominated by dense glass with blocky shapes that commonly display stepped surfaces (Figures 10a and 10c), representing fragmentation processes of comparably much higher deformation energy density. In addition, some of the particles show quenched crack structures (Figure 10e), acquired at the time of fragmentation by fast acceleration and simultaneous quenching of a newly fragmented particle through a liquid water domain [e.g., *Büttner et al.*, 1999, 2002]. These features are all typical of phreatomagmatic fragmentation and have already been documented to result from experimentally generated basaltic MFCI. The same textural features occur in natural particles from lower-sequence deposits at Tepexitl (Unit 2; Figures 10b, 10d, and 10f), additional evidence that phreatomagmatic processes powered early explosive eruptions at Tepexitl. We interpret this nearly identical particle morphology as evidence that such natural processes were similar to magma-water interaction processes as observed during the WE experiments.

6. Conclusions

[19] Explosive magma-water interactions were generated under laboratory conditions using remelted rhyolite rock from Tepexitl volcano in Mexico. Analyses of both physical parameters during experiments and particles produced by the experiments clearly show that MFCI occurred during experiments, with resulting products clearly distinguished from products of experiments not involving magma-water interaction. Additionally, comparative analysis of ash grains from Tepexitl deposits (lower-sequence Unit 2) revealed that MFCI was one of the driving mechanisms for early eruptions at Tepexitl.

[20] The distinguishing features of active phreatomagmatic particles found in the ash fraction of the Tepexitl samples were nearly identical to those found in phreatomagmatic deposits of many basaltic, andesitic, and trachytic eruptions [e.g., *Dellino and La Volpe*, 1996; *Dellino et al.*, 2001; *Büttner et al.*, 2002]. Thus, the same methods of discrimination between phreatomagmatic and magmatic fragmentation processes for mafic melts can be used for the products of high-silica explosive eruptions.

[21] The difference between the geometrical configurations for basaltic and rhyolitic MFCI experiments conducted

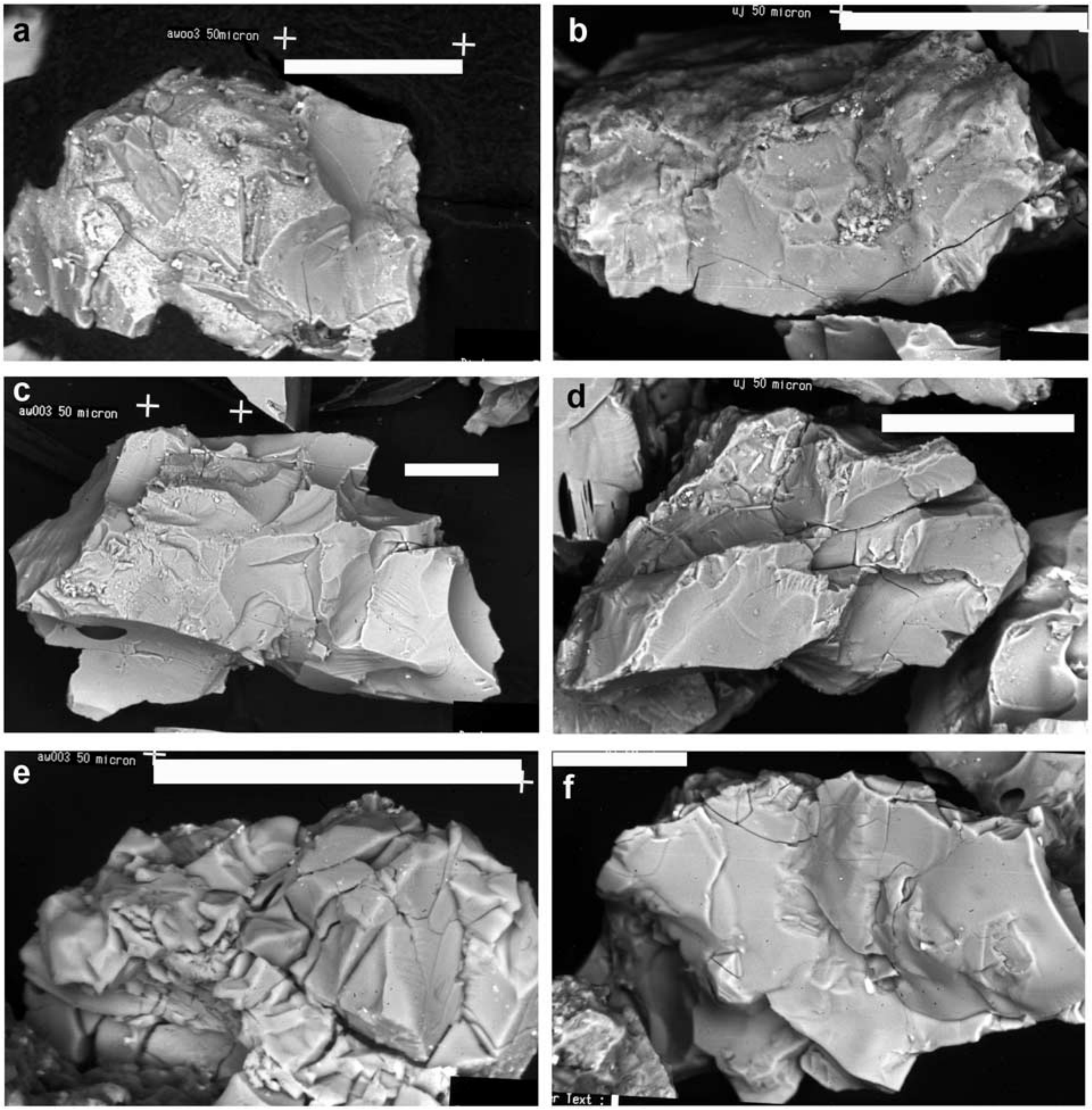

Figure 10. (a, c, and e) Ash particles from WE runs and (b, d, and f) particles from natural phreatomagmatic deposits of Tepexitl. Scale bar is 50 μm.

in our laboratory lies in the conditions of initial contact between melt and water (the premix phase). In basaltic experiments, water is injected into the melt, whereas in rhyolite experiments, water is released on top of the melt. Although this initial interface/volume ratio area of the rhyolite melt and water does not allow for the heat transfer needed to achieve explosive MFCI conditions, fracturing caused by contemporary ''magmatic'' fragmentation (induced by deformation of the melt) increased the interfacial surface area, thus triggering phreatomagmatic explosions. Ascent of high-silica magma most likely will cause deformational stress leading to superficial fracturing, as demonstrated by numerous observations [e.g., *Tuffen et al.*, 2003; *Rust et al.*, 2004; *Castro et al.*, 2005; *Gonnermann and Manga*, 2005]. These fractures appear to be essential in generating conditions needed for high-silica MFCI, which suggests that magmatic processes can trigger phreatomagmatic explosions of rhyolitic and dacitic magma.

[22] The evidence presented in this first comparative rhyolitic study can be used to enhance our understanding of potential hazards in provinces of dacitic-rhyolitic volcanism. In such a high-silica volcanic area, the presence of shallow aquifers, unconsolidated and water saturated sediments, and/or development of superficial hydrothermal systems may indicate the potential for high-energy pyroclastic activity. Strong precipitation events [e.g., *Mastin*, 1994, *Elsworth et al.*, 2004], melting of ice caps, or drastic

changes in the superficial groundwater circulation [*Wohletz and Heiken*, 1992; *Dadd and Van Wagoner*, 2002; *Gutmann*, 2002] may cause a change of the eruptive behavior from effusive to explosive eruptions.

[23] **Acknowledgments.** Support for the experimental work was provided by the College of Engineering and Natural Sciences and the Department of Geology at Northern Arizona University. Support for Erickson's research stay in Würzburg was provided by a J. William Fulbright Grant. Many thanks to Greg Valentine, Ken Wohletz, Larry Mastin, and the associate editor Andre Revil; their insightful and constructive reviews were a great help in improving this paper.

References

Austin-Erickson, A. (2007), Phreatomagmatic eruptions of rhyolitic magma: A case study of Tepexitl tuff ring, Serdan-Oriental Basin, Mexico, 194 pp., M.S. thesis, N. Ariz. Univ., Flagstaff.

Brooker, M. R., B. F. Houghton, C. J. N. Wilson, and J. A. Gamble (1993), Pyroclastic phases of a rhyolitic dome-building eruption; Puketarata tuff ring, Taupo volcanic zone, New Zealand, *Bull. Volcanol.*, *55*, 395–406, doi:10.1007/BF00301999.

Büttner, R., and B. Zimanowski (1998), Physics of thermohydraulic explosions, *Phys. Rev. E*, *57*, 5726–5729, doi:10.1103/PhysRevE.57.5726.

Büttner, R., P. Dellino, and B. Zimanowski (1999), Identifying modes of magma/water interaction from the surface features of ash particles, *Nature*, *401*, 688–690, doi:10.1038/44364.

Büttner, R., P. Dellino, L. LaVolpe, V. Lorenz, and B. Zimanowski (2002), Thermohydraulic explosions in phreatomagmatic eruptions as evidenced by the comparison between pyroclasts and products from Molten Fuel Coolant Interaction experiments, *J. Geophys. Res.*, *107*(B11), 2277, doi:10.1029/2001JB000511.

Büttner, R., P. Dellino, H. Raue, I. Sonder, and B. Zimanowski (2006), Stress induced brittle fragmentation of magmatic melts: Theory and experiments, *J. Geophys. Res.*, *111*, B08204, doi:10.1029/2005JB003958.

Campos Venuti, M., and P. L. Rossi (1996), Depositional facies in the Fyriplaka rhyolitic Tuff Ring, Milos Island (Cyclades, Greece), *Acta Vulcanol.*, *8*(2), 173–190.

Carrasco-Núñez, G., M. H. Ort, and C. Romero (2007), Evolution and hydrological conditions of a maar volcano (Atexcac crater, Eastern Mexico), *J. Volcanol. Geotherm. Res.*, *159*(1–3), 179–197, doi:10.1016/j.jvolgeores.2006.07.001.

Castro, J. M., D. B. Dingwell, A. R. L. Nichols, and J. E. Gardner (2005), New insights on the origin of flow bands in obsidian, *Geol. Soc. Am. Spec. Pap.*, *396*, 55–65.

Dadd, K. A., and N. A. Van Wagoner (2002), Magma composition and viscosity as controls on peperite texture: An example from Passamaquoddy Bay, southeastern Canada, *J. Volcanol. Geotherm. Res.*, *114*, 63–80, doi:10.1016/S0377-0273(01)00288-8.

Dellino, P., and L. La Volpe (1995), Fragmentation versus transportation mechanisms in the pyroclastic sequence of Monte Pilato-Rocche Rosse (Lipari, Italy), *J. Volcanol. Geotherm. Res.*, *64*, 211–231, doi:10.1016/0377-0273(94)00084-T

Dellino, P., and L. La Volpe (1996), Image processing analysis in reconstructing fragmentation and transportation mechanisms of pyroclastic deposits: The case of Monte Pilato-Rocche eruptions, Lipari (Aeolian Island, Italy), *J. Volcanol. Geotherm. Res.*, *71*, 13–29, doi:10.1016/0377-0273(95)00062-3.

Dellino, P., R. Isaia, L. La Volpe, and G. Orsi (2001), Statistical analysis of textural data from complex pyroclastic sequences: Implications for fragmentation processes of the Agnano Monte Spina Tephra (4.1 ka), *Phlegraean Fields, southern Italy, Bull. Volcanol.*, *63*(7), 443–461, doi:10.1007/s004450100163.

Elsworth, D., B. Voight, G. Thompson, and S. R. Young (2004), Thermal-hydraulic mechanism for rainfall-triggered collapse of lava domes, *Geology*, *32*(11), 969–972, doi:10.1130/G20730.1.

Gonnermann, H. M., and M. Manga (2005), Flow banding in obsidian; a record of evolving textural heterogeneity during magma deformation, *Earth Planet. Sci. Lett.*, *236*(1–2), 135–147, doi:10.1016/j.epsl.2005.04.031.

Gutmann, J. T. (2002), Strombolian and effusive activity as precursors to phreatomagmatism; eruptive sequence at maars of the Pinacate volcanic field, Sonora, Mexico, *J. Volcanol. Geotherm. Res.*, *113*(1–2), 345–356, doi:10.1016/S0377-0273(01)00265-7.

Heiken, G. H., and K. Wohletz (1987), Tephra deposits associated with silicic domes and lava flows, *Geol. Soc. Am. Spec. Pap*, *212*, 55–76.

Houghton, B. F., and H.-U. Schmincke (1986), Mixed deposits of simultaneous strombolian and phreatomagmatic volcanism: Rothenberg volcano, East Eifel volcanic field, *J. Volcanol. Geotherm. Res.*, *30*, 117–130.

Houghton, B. F., C. J. N. Wilson, and S. D. Weaver (1987), The Opo Bay tuff cone, Mayor Island; interaction between rising gas-poor pantelleritic magma and external water, *N. Z. Geol. Surv.*, *18*, 79–85.

Kazuhiko, K., O. Takeshi, H. Shintaro, U. Kozo, and T. Danhara (2002), Toga Volcano: An Alkali-Rhyolite tuff-ring in the Western end of Oga Peninsula, NE Japan, *Bull. Volcanol. Soc. Jpn.*, *47*, 373–396.

Lorenz, V. (1985), Maars and diatremes of phreatomagmatic origin, a review, *Trans. Geol. Soc. S. Afr.*, *88*, 459–470.

Lorenz, V. (1986), On the growth of maars and diatremes and its relevance to the formation of tuff-rings, *Bull. Volcanol.*, *48*, 265–274, doi:10.1007/BF01081755.

Lorenz, V. (1987), Phreatomagmatism and its relevance, *Chem. Geol.*, *62*, 149–156, doi:10.1016/0009-2541(87)90066-0.

Lorenz, V., and J. Haneke (2004), Relationships between diatremes, dykes, sills, laccoliths, intrusive-extrusive domes, lava flows, and tephra deposits with unconsolidated water-saturated sediments in the late Variscan intermontane Saar-Nahe Basin, SW Germany, *Geol. Soc. Spec. Publ.*, *234*, 75–124.

Mastin, L. G. (1994), Explosive tephra emissions at Mount St. Helens, 1989–1991: The violent escape of magmatic gas following storms?, *Geol. Soc. Am. Bull.*, *106*, 175–185.

Morrisey, M., B. Zimanowski, K. Wohletz, and R. Büttner (2000), Phreatomagmatic fragmentation, in *Encyclopedia of Volcanoes*, edited by H. Sigurdsson, pp. 431–445, Academic, London.

Pier, J. G., J. F. Luhr, F. A. Podosek, and J. J. Aranda-Gómez (1992), The La Breña—El Jagüey Maar Complex, Durango, Mexico: II. Petrology and geochemistry, *Bull. Volcanol.*, *54*(5), 405–428, doi:10.1007/BF00312322.

Rust, A. C., K. V. Cashman, and P. J. Wallace(2004), Magma degassing buffered by vapor flow through brecciated conduit margins, *Geology*, *32*(4), 349–352, doi:10.1130/G20388.2.

Self, S., and R. S. J. Sparks (1978), Characteristics of widespread pyroclastic deposits formed by the interaction of silicic magma and water, *Bull. Volcanol.*, *41*, 196–212, doi:10.1007/BF02597223

Sheridan, M. F., and R. G. Updike (1975), Sugarloaf Mountain Tephra— A Pleistocene rhyolitic deposit of base-surge origin in northern Arizona, *Geol. Soc. Am. Bull.*, *86*(4), 571–581.

Siebe, C., and S. P. Verma (1988), Major element geochemistry and tectonic setting of Las Derrumbadas rhyolitic dome, Puebla, Mexico, *Chem. Erde*, *48*(3), 177–189.

Siebe, C., M. Abrams, and M. F. Sheridan (1993), Major Holocene block-and-ash fan at the western slope of ice-capped Pico de Orizaba Volcano, Mexico; implications for future hazards, *J. Volcanol. Geotherm. Res.*, *59*, 1–33, doi:10.1016/0377-0273(93)90075-3.

Siebert, L., and G. Carrasco-Núñez (2002), Late-Pleistocene to precolumbian behind-the arc mafic volcanism in the eastern Mexican Volcanic Belt; implications for future hazards, *J. Volcanol. Geotherm. Res.*, *115*, 179–205, doi:10.1016/S0377-0273(01)00316-X.

Sieh, K., and M. I. Bursik (1986), Most recent eruption of the Mono Craters, eastern Central California, *J. Geophys. Res.*, *91*(B12), 12,539–12,571, doi:10.1029/JB091iB12p12539>.

Tuffen, H., D. B. Dingwell, and H. Pinkerton (2003), Repeated fracture and healing of silicic magma generate flow banding and earthquakes?, *Geology*, *31*(12), 1089–1092, doi:10.1130/G19777.1.

White, J. D. L. (1991), Maar-diatreme phreatomagmatism at Hopi Buttes, Navajo Nation (Arizona) U.S.A, *Bull. Volcanol.*, *53*, 239–258, doi:10.1007/BF00414522.

White, J. C., and K. M. Urbanczyk (2002), The Pine Canyon Rhyolite: A newly recognized occurrence of pantellerite in Big Bend National Park, Texas, paper presented at 36th Annual Meeting, Geol. Soc. of Am., Boulder, Colo.

Wohletz, K. H. (1983), Mechanisms of hydrovolcanic pyroclast formation: Grain-size, scanning electron microscopy, and experimental studies, *J. Volcanol. Geotherm. Res.*, *17*, 31–64, doi:10.1016/0377-0273(83)90061-6.

Wohletz, K. H. (1986), Explosive magma-water interactions: Thermodynamics, explosion mechanisms, and field studies, *Bull. Volcanol.*, *48*, 245–264, doi:10.1007/BF01081754 1986.

Wohletz, K. H., and G. Heiken (1992), *Volcanology and Geothermal Energy*, 432 pp., Univ. of Calif. Press, Berkeley.

Zimanowski, B. (1998), Phreatomagmatic explosions, in *From Magma to Tephra*, edited by A. Freundt and M. Rosi, pp. 25–54, Elsevier, New York.

Zimanowski, B., and R. Büttner (2003), Phreatomagmatic explosions in subaqueous eruptions, in *Explosive Subaqueous Volcanism*, *Geophys. Monogr. Ser. vol.* 140, edited by J. D. L. White, J. L. Smellie, and D. Clague, pp. 51–60, AGU, Washington, D. C.

Zimanowski, B., G. Fröhlich, and V. Lorenz (1991), Quantitative experiments on phreatomagmatic explosions, *Volcanol. Geotherm. Res*, *48*, 341–358, doi:10.1016/0377-0273(91)90050-A.

Zimanowski, B., R. Büttner, V. Lorenz, and H.-G. Häfele(1997a), Fragmentation of basaltic melt in the course of explosive volcanism, *J. Geophys. Res.*, *102*, 803–814, doi:10.1029/96JB02935.

Zimanowski, B., R. Büttner, and V. Lorenz (1997b), Premixing of magma and water in MFCI experiments, *Bull. Volcanol.*, *58*, 491–495, doi:10.1007/s004450050157.

Zimanowski, B., K. H. Wohletz, R. Büttner, and P. Dellino, The volcanic ash problem (2003b), *J. Volcanol. Geotherm. Res.*, *122*, 1–5, doi:10.1016/S0377-0273(02)00471-7.

Zimanowski, B., R. Büttner, and A. Koopmann (2004), Experiments on magma mixing, *Geophys. Res. Lett.*, *31*, L09612, doi:10.1029/2004GL019687.

A. Austin-Erickson and M. H. Ort, Department of Geology, Northern Arizona University, Flagstaff, AZ 86011, USA.

R. Büttner and B. Zimanowski, Physikalisch Vulkanologisches Labor, Universität Würzburg, D-97070 Würzburg, Germany. (zimano@mail.uni-wuerzburg.de)

P. Dellino, Dipartimento Geomineralogico, Università Degli Studi di Bari, I-70125 Bari, Italy.